scientific reports

Check for updates

OPEN

Research and application on modeling and landing point prediction technology for water jet trajectory of fire trucks under large-scale scenarios

Qing Fan[1✉], Qianwang Deng[1] & Qin Liu[2]

To let water jets land at the fire, pitch angle of the fire monitor has to be adjusted manually with successive rounds, which seriously affects the efficiency of fire extinguishing. To improve the efficiency, this paper proposes a technology for water jet trajectory modeling and landing point prediction to help with extinguishing automatically. Considering fragmentation and atomization of water jets, trajectories are analyzed and the predicted trajectory is closer to the real situation. Secondly, a compensation method for the prediction is proposed to further reduce the deviation between the predicted and the actual landing point, taking into account the combined effects of high altitude, initial jet velocity, and wind. On this basis, considering the difficulty of directly solving the analytical solution to the target initial pitch angle of the jets, a searching method is also proposed, which greatly improves the solving efficiency. Finally, through practical experiments and verification, the proposed model takes an average time of 0.00292 s, which is far less compared with other methods. The prediction error is improved by at least 45.3%, and the average deviation is less than 2 m.

The intelligent fire monitor is a significant appliance through the development of fire distinguishing system, which aims and shoots automatically. Whether the fire is to be distinguished is up to the aiming accuracy, hence it is the destination of jets that this paper is concerned about.

The trajectory of water jets is like a parabola before jets hit the ground or other targets since ejection. The exact trajectory depends on the real-time force condition that water jets are under, which usually consists of monitor thrust, air resistance, gravity and other forces, which determines the landing point. Moreover, the initial force condition depends on the pitch angle of the monitor, which initializes the counterbalance between forces at the beginning. In other words, it is able to adjusting the jet range by adjusting the initial pitch angle of the monitor. Once the jet range is decided, the corresponding initial pitch angle is supposed to be obtained and applied. As a result, to achieve the intelligent fire water monitors, it can be done by pitch angle adjustment that water jets land at which the fire locates at.

The trajectory model and landing point prediction is the basis of pitch angle adjustment automation. Whether a monitor can point to the fire is closely related to the prediction precision, influencing distinguishing efficiency. Consequently, trajectory model and landing point prediction is an important subject in the process of intelligent distinguishing system development, which former researchers have already conducted some, mainly about 3 categories of solution: prediction using neural network[1–4], modeling using classical mechanics[5–8], and modeling using fluid dynamic methodology[9,10].

Neural network, known for its human-alike characteristics of hierarchical cognition, is widely applied in recent years[1]. To predict the landing point, Hao[11] and other researchers[2] proposed trajectory models of water jets, which use BP neural networks combined with the genetic algorithm to solve. However, when a neural network

[1]College of Mechanical and Vehicle Engineering, Hunan University, Changsha 410000, China. [2]Central Research Center, Zoomlion Heavy Industry Science & Technology Co., Ltd, Changsha 410000, China. ✉email: fqzlzk@163.com

1

comes into the training of landing point prediction, it is hard to exploit its advantage from a small and limited dataset, from which it is difficult for it to get an accurate landing point. Moreover, performance of the genetic algorithm depends on the chromosome coding, population size, iteration times and other super-parameters, which makes difficult to balance between high precision and large computation complexity that takes a lot of time. Thus, Lin et al.[3] fitted a linear prediction model under ideal condition at first and then updated coefficients of the model by BP neural network, which saves a lot of time but hard to be applied in other complex environments.

The ideal condition without air resistance named in the field of classical mechanics barely exists in real situation, especially in emergency response system. Therefore, Chen et al.[7] considered the influence of the air resistance on the trajectory of water jets and he assumed the magnitude of air resistance was proportional to velocity. Min et al.[8] believed that the air resistance was related to the initial pitch angle. A different pitch angle brings a different horizontal velocity and a different vertical velocity, thus a different air resistance magnitude coefficient in horizontal and in vertical direction respectively. However, Sun[9] thought fragmentation of water jets would stop them from modeling a precise trajectory even though they already considered air resistance, and he proposed a jet trajectory with the help of Fluent, which is a popular computational fluid dynamics(CFD) tool, considering jets fragmentation and the monitor's internal structure, though the range error still reached around 10%.

The movement of water jets can also be explained by hydrodynamics. Sun[9] simulated it by Fluent, while Zhu[10] simulated it by a moving particle semi-implicit method(MPS), in which the movement for each particle at the moment is updated by coupling relation between particles at the last moment and every movement at any time becomes accessible step by step. Indeed, predicting the landing point supported by hydrodynamics brings a high precision. Nevertheless, its computation costs lots of time, extremely hard to meet the emergency requirement of quick response. As a result, it is normally applied in model validation instead of in real-time computation.

Above all, the precision and the time efficiency of jet landing point prediction in the field of emergency firefighting are continued to be upgraded. This paper proposes a jet trajectory model under large-scale scenarios, which updates the classical jet trajectory reference to the fragmentation and air resistance and also proposes a compensation method for landing point prediction, which greatly improves the accuracy without increasing time conspicuously. This paper considers the magnitude of air resistance to be just proportional to the velocity, unlike Min and other researcher's study[8], the air resistance coefficient for each direction remains the same. It is the influence of fragmentation on water trajectory that this paper mainly focuses on, using a core stable jet coefficient to represent the change of trajectory after jets crushing, which performs well in the experiments. At the end, this paper also generates a system to predict the initial pitch angle to help with emergent firefighting, which is illustrated in Fig. 1.

Water jet trajectory modeling
Water jet trajectory considering air resistance

The water jet movement in the air can be seen as a special projectile motion too. Considering gravity and air resistance instead of fragmentation and other influence, the movement is almost compliant with the characteristics noted in Newton's Second Law.

Normally, there are 2 statements about the magnitude of air resistance, which are that the magnitude is directly proportional to velocity[12] and that proportional to the square of velocity[8,9].

Proportional to velocity
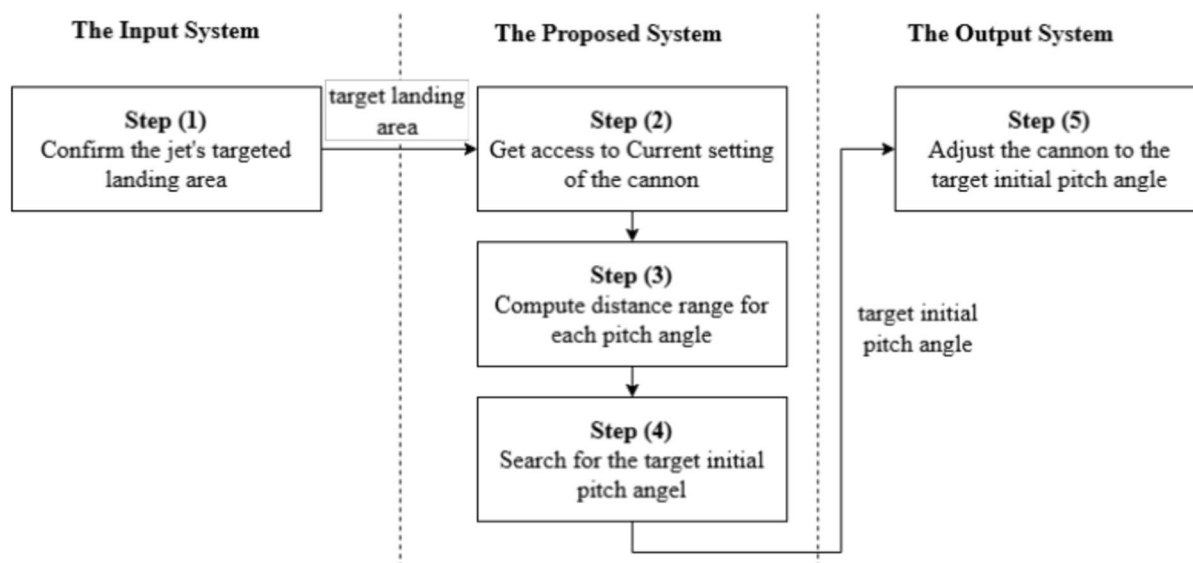That the air resistance is proportional to velocity is represented by Eq. (1).

Fig. 1. Process of cannon controlling.

$$F = k \cdot \vec{v} \tag{1}$$

After force decomposing, the velocity $v_{x,t}$ in horizontal direction, which is represented by x, at the time of t can be denoted as Eq. (2).

$$v_{x,t} = v_{x,t-1} - \frac{k}{m} \cdot v_{x,t-1} \cdot \Delta t \tag{2}$$

while jetting upwards, the velocity $v_{y,t}$ in vertical direction, which is represented by y, at the time t can be denoted as Eq. (3),

$$v_{y,t} = v_{y,t-1} + \left(-g_n - \frac{k}{m} \cdot v_{y,t-1} \right) \cdot \Delta t \tag{3}$$

Thus, the displacement of x and y at t is represented by Eq. (4).

$$\begin{cases} x_t = x_{t-1} + \frac{v_{x,t} + v_{x,t-1}}{2} \cdot \Delta t \\ y_t = y_{t-1} + \frac{v_{y,t} + v_{y,y-1}}{2} \cdot \Delta t \end{cases} \tag{4}$$

From 1 to 4 above, m denotes the gravity of water jets, k denotes the coefficient of air resistance, Δt denotes the time unit, and g_n denotes the gravitational acceleration.

To let x directly correspond to t, Eq. (2) can be transformed to:

$$-\frac{m}{k \cdot v_x} \Delta v_x = \Delta t \tag{5}$$

Assuming a water jet weighted m ejects at speed v_{out} at a pitch angle θ ($\theta > 0$ means ejecting upwards while $\theta < 0$ means ejecting downwards), which is $x_0 = 0, y_0 = H_0, v_{0x} = v_{out} \cdot \cos\theta, v_{0y} = v_{out} \cdot \sin\theta$. Integrate Eq. (5) over time $(0, t)$, then get Eq. (6).

$$\int_0^t \int_{v_{out}\cos\theta}^{v_x} -\frac{m}{k \cdot v_x} dv_x dt = \int_0^t \int_0^t dt dt \tag{6}$$

Similarly, y can also be solved, thus the trajectory can be represented as:

$$\begin{cases} x = \frac{m \cdot v_{out} \cdot \cos\theta \cdot \left(1 - e^{-\frac{kt}{m}}\right)}{k} \\ y = \frac{(m^2 g_n + m \cdot k \cdot v_{out} \cdot \sin\theta)\left(1 - e^{-\frac{kt}{m}}\right) - mg_n kt}{k^2} + H_0 \end{cases} \tag{7}$$

where H_0 is the height where jets eject, briefly named as the initial ejecting height.

Proportional to the square of velocity
That the air resistance magnitude is proportional to velocity is defined by Eq. (8).

$$F = k \cdot \|v_{t-1}\| \cdot \vec{v} \tag{8}$$

Similarly, the velocity v_{xt} is defined as: $v_{x,t} = v_{x,t-1} - \frac{k}{m} \cdot \|v_{t-1}\| \cdot \Delta t$

If jetting upwards, the velocity $v_{y,t}$ is defined as:

$$v_{y,t} = v_{y,t-1} + \left(-g_n - \frac{k}{m} \cdot \|v_{t-1}\| \cdot v_{y,t-1} \right) \cdot \Delta t \tag{9}$$

And if jetting downwards, the $v_{y,t}$ is defined as:

$$v_{y,t} = v_{y,t-1} + \left(-g_n + \frac{k}{m} \cdot \|v_{t-1}\| \cdot v_{y,t-1} \right) \cdot \Delta t \tag{10}$$

so, the velocity v_t is defined as:

$$\|v_{t-1}\| = \sqrt{v_{x,t-1}^2 + v_{y,t-1}^2} \tag{11}$$

the displacement of x and y is defined as:

$$\begin{cases} x_t = x_{t-1} + \frac{v_{x,t} + v_{x,t-1}}{2} \cdot \Delta t \\ y_t = y_{t-1} + \frac{v_{y,t} + v_{y,t-1}}{2} \cdot \Delta t \end{cases} \tag{12}$$

From Eqs. (8 to 12), m is the gravity of water jets, k denotes the coefficient of air resistance, Δt denotes the time unit, and g_n denotes the gravitational acceleration.

Though the integral of Eq. (12) cannot be parsed directly, similar to Eq. (7), it can be reasonably inferred that under certain condition of m and k, x and y are only corresponding to v_{out} and θ.

However, as is said before, the ideal condition that only considers air resistance and gravity barely exists in real world. The classical jet trajectory defined in Eqs. 4 and in 12 are still far away from the real trajectory. One of the causes lies in the fact that the process from jet ejecting to landing is concluded to 3 stages, which is the stability stage, the decline stage and the crushing stage. In the stage of stability, there is a region of supersonic flow with constant velocity at the cannon nozzle outlet, where the axial shaft line velocity and density of jets basically remain unchanged and the formation of jets is stable, insusceptible of wind and others. In stage decline, affected by air resistance, water jets' axial shaft line velocity declines regularly and the part far from the axis of jet deviates the axis gradually, though the formation is still quite stable, which is totally different from stage crushing, where the velocity decreases violently, jets crush into water droplets and mix up with the air, susceptible to air resistance, wind and other influences.

As is illustrated in Fig. 2, at the end of trajectory, its fragmentation makes it vulnerable, thus it becomes easier for jets to be affected by air resistance and wind. Consequently, the landing area expands, the landing happens earlier and the range is closer, compared to the landing under ideal condition.

Regarding to these characteristics, Min et al.[8] updated the jet movement model starting from the coefficient of air resistance. However, his adaptation is hard to be executed in a practical application, it triggers off this paper though.

Jet trajectory proposed

The movement of jets consists of upward movement and downward movement, from ejecting to landing. Moving upwards means that at time t, the direction θ_t of velocity v is greater than 0, while moving downwards means $\theta_t < 0$. Considering that air resistance direction is opposite to the movement direction, these 2 movements are discussed respectively.

Jet trajectory based on core stable jets during moving upward

In the classical jet trajectory models defined by Eqs. 4 and 12, during moving upward, jets receive steadily negative affection from air resistance and gravity, which decreases the vertical velocity uniformly. However, it is contrary to the facts that the vertical velocity decreases with a accelerated acceleration, pushing jets fast into crushing stage where the force condition changes extremely and that the acceleration undergoes a qualitative change. Meanwhile, the horizontal direction of jets is also affected by air resistance negatively, of which the acceleration is far smaller than of the vertical direction. Thus, the impact to the horizontal acceleration is negligible. To conclude, in the process of moving forward, vertical acceleration increases gradually and the formation becomes unstable, which affects the acceleration in return, which repeats until jets crush totally or the vertical velocity meets 0.

As a result, a definition of core stable jets , which are the parts from the jet ejection to the last time before its crush begins, is proposed. During upward movement, it is mainly represented by the vertical displacement, directly affecting vertical velocity. Thus, the proposed upward movement is:
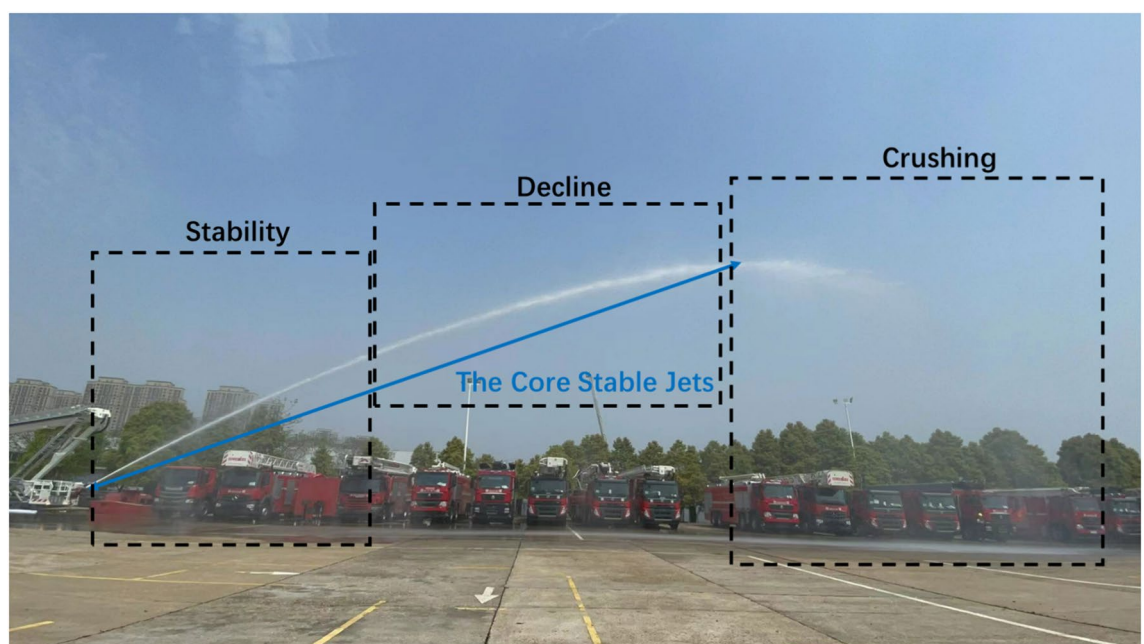

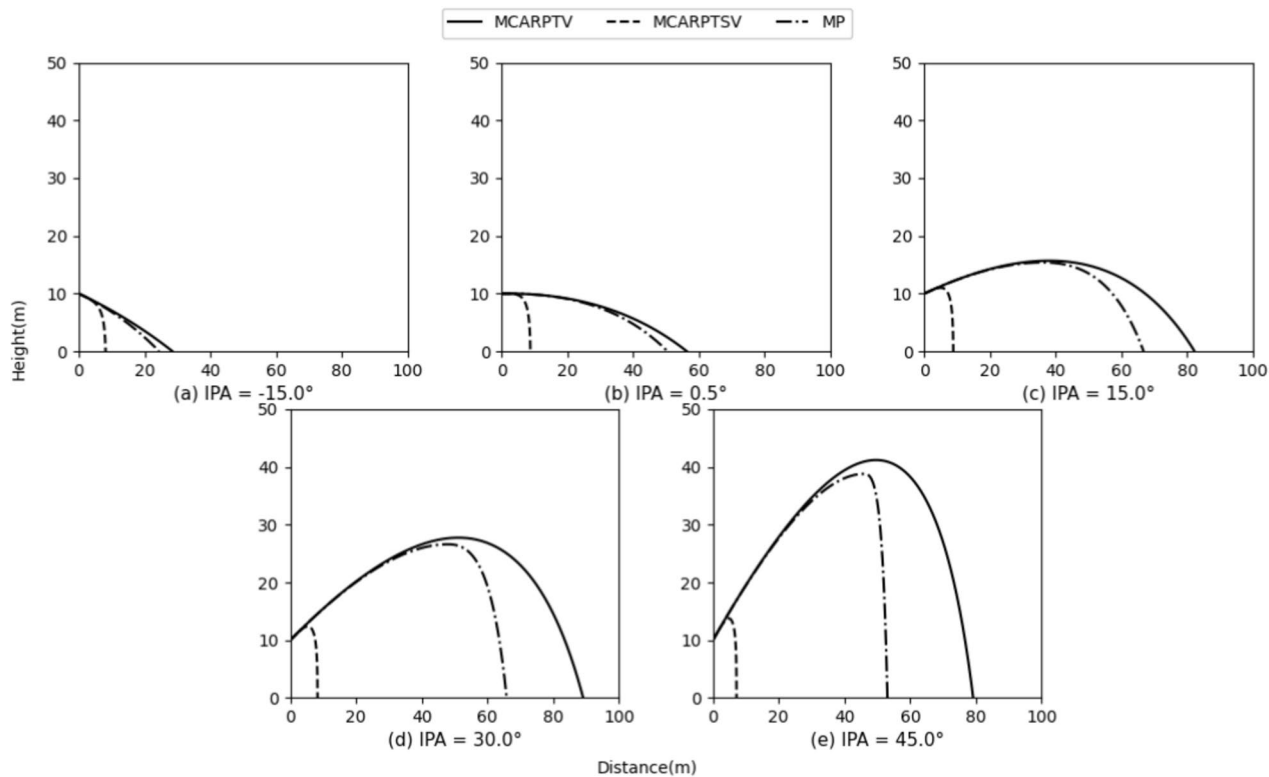**Fig. 2.** Process of cannon controlling.

Fig. 3. Water jet trajectory computed by models. *IPV* represents the initial pitch angle, *MCARPTV* represents the model considering air resistance proportional to velocity, *MCARPTSV* represents the model considering air resistance proportional to the square of velocity, *MP* represents the model proposed.

Initial pitch angle (IPA)	Model considering air resistance proportional to velocity (MCARPTV)		Model considering air resistance proportional to the square of velocity (MCARPTSV)		Model proposed (MP)	
	Height range	Distance range	Height range	Distance range	Height range	Distance range
-20.00	22.79	–	7.82	–	20.01	–
-15.00	28.38	–	8.14	–	24.40	–
0.50	56.33	10.01	8.77	10.01	50.50	10.01
15.00	82.04	15.69	8.83	11.01	66.71	15.40
30.00	89.00	27.75	8.31	12.40	65.85	26.60
45.00	79.14	41.19	7.18	13.78	53.08	38.79

Table 1. Distance range and height range predicted by models.

$$\begin{cases} v_{x,t} = v_{x,t-1} - \frac{k}{m} \cdot v_{x,t-1} \cdot \Delta t \\ v_{y,t} = v_{y,t-1} + \left(-g_n - \frac{k}{m} \cdot v_{y,t-1} - \sigma_u \cdot y_{t-1}\right) \cdot \Delta t \\ x_t = x_{t-1} + \frac{(v_{x,t}+v_{x,t-1})}{2} \cdot \Delta t \\ y_t = y_{t-1} + \frac{(v_{y,t}+v_{y,t-1})}{2} \cdot \Delta t \end{cases} \tag{13}$$

where $\sigma_u (\sigma_u > 0)$ is a super-parameter, representing the impact degree of core stale jets on vertical velocity. Thus, the larger vertical displacement is, the larger vertical velocity is, in line with the reality.

Jet trajectory based on core stable jet combined with integrated coefficient during moving downward
During moving downward, vertical velocity receives a positive impact from gravity and a negative impact from air resistance, hence the acceleration is smaller than of moving upward, resulting a longer movement. Thus, core stable jets' impact on horizontal velocity is not negligible. However, compared to its impact in upward movement, the impact in downward movement is smaller due to the smaller acceleration. Hence, the proposed downward movement is represented as:

$$\begin{cases} v_{x,t} = v_{x,t-1} - \left(\frac{k}{m} \cdot v_{x,t-1} + \sigma_x \cdot y_{t-1} \cdot \frac{v_{x,t-1}}{\|v_{y,t-1}\|} \right) \cdot \Delta t \\ v_{y,t} = v_{y,t-1} + \left(-g_n + \frac{k}{m} \cdot v_{y,t-1} - \sigma_d \cdot y_{t-1} \right) \cdot \Delta t \\ x_t = x_{t-1} + \frac{(v_{x,t}+v_{x,t-1})}{2} \\ y_t = y_{t-1} + \frac{(v_{y,t}+v_{y,t-1})}{2} \end{cases} \tag{14}$$

where $\sigma_d (0 < \sigma_d < \sigma_u)$ and $\sigma_x (0 < \sigma_x)$ are super-parameters, representing the influence of core stable jets on vertical velocity and on horizontal velocity respectively; θ_t represents the pitch angle of water jets at time t; $v_{y,t-1}$ and $v_{x,t-1}$ represent the vertical velocity and the horizontal velocity at time $(t-1)$ respectively and $\|\cdot\|$ represents the mode.

Landing point prediction and pitch angle computation

Wang et al.[13] and Wang et al.[14] reached a landing point by an equation respectively, and Hao[11] used neural network to predict a landing point. None of these prediction methods are suitable for this paper, since it is too complex to solve Eq. (14). As a result, this paper decides to follow Liu et al.[15] to solve Eq. (14) iteratively rather than an one-step formula.

As a result, this paper compares the landing points $\{x_t, y_t | y_t = 0\}$ obtained by Eqs. (4, 12 and 14) and Fig. 3 shows their results respectively, and the results are valued as Table 1. The initial ejecting height is 10 m, the working water pressure is 0.9 mPa and the initial pitch angle includes $-15°, 0°, 15°, 30°$ and $45°$. As is shown in Table 1, the jet height range computed by the model considering air resistance measured directly by velocity is from 10 to 41.2 m, and the jet distance range is from 22.8 to 89 m. Its biggest height range happens at pitch angle $45°$ and biggest distance range happens at pitch angle $30°$. The height range varies from 5 to 31 m and the distance range varies from 5 to 56 m. The figure of its trajectory is quite symmetrical. The jet height range computed by the model considering air resistance measured by the square of velocity is from 10 to 13.8 m, and the jet distance range is from 7.8 to 8.9 m. Its biggest height range happens at pitch angle $45°$ and biggest distance range happens at pitch angle $15°$. The height range varies from 1 to 4 m and the distance range varies from 0.5 to 2 m. The figure of its trajectory is dramatically unsymmetrical, and it is just like falling down straightly before y hits 0. The jet height range computed by the model proposed in this paper is from 10 to 38.8 m, and the jet distance range is from 20 to 66.8 m. Its biggest height range happens at pitch angle $45°$ and biggest distance range happens at pitch angle $15°$. The height range varies from 5 to 29 m and the distance range varies from 4 to 46 m. The figure of its trajectory is relatively unsymmetrical and it is like a straight falling before the hit when
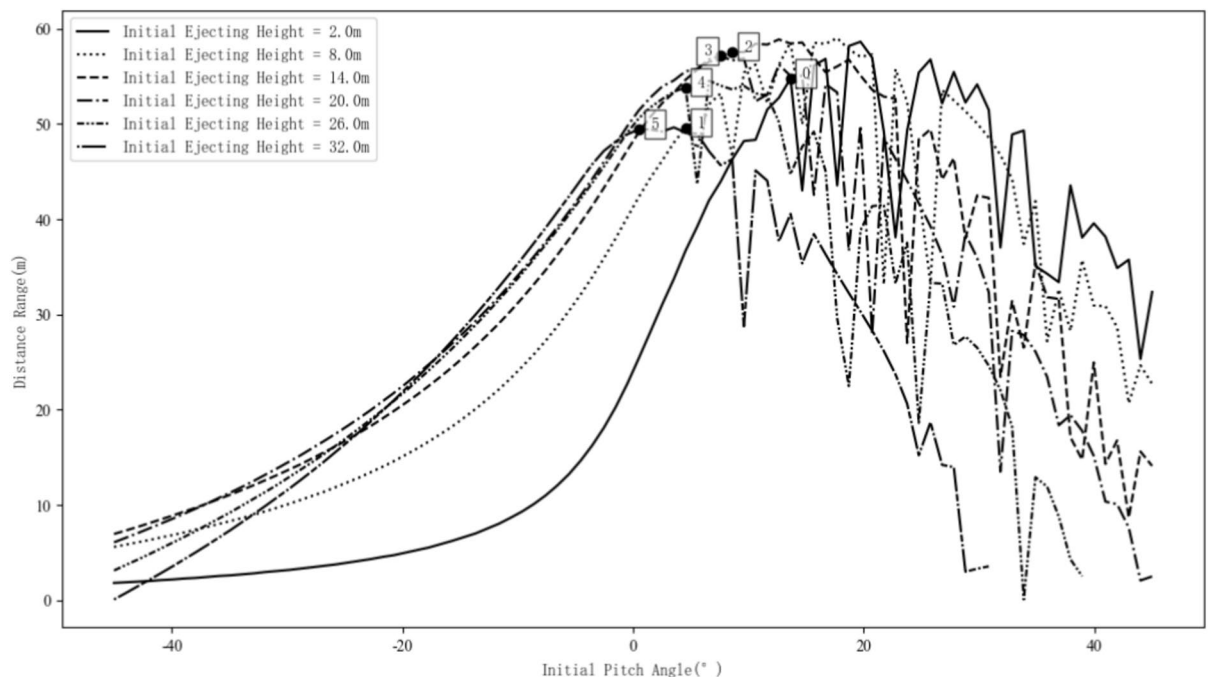

Fig. 4. The variation of distance range with initial pitch angle. 0. When the initial ejecting height is 2.0 m, the max distance range is 54.8 m and the corresponding initial pitch angle is 13.7° 1. When the initial ejecting height is 8.0 m, the max distance range is 49.6 m and the corresponding initial pitch angle is 4.6° 2. When the initial ejecting height is 14.0 m, the max distance range is 57.6 m and the corresponding initial pitch angle is 8.6° 3. When the initial ejecting height is 20.0 m, the max distance range is 57.1 m and the corresponding initial pitch angle is 7.6° 4. When the initial ejecting height is 26.0 m, the max distance range is 53.8 m and the corresponding initial pitch angle is 4.6° 5. When the initial ejecting height is 32.0 m, the max distance range is 49.4 m and the corresponding initial pitch angle is 0.5°.

6

the pitch angle is quite large. From the point of view of trajectory characteristics, the proposed model matches best to the real trajectory in Fig. 2.

The compensation of landing point prediction based on samples

In practical application, errors still happen under some special conditions if predicting the landing point directly by the proposed model due to the different influence of complex environments, which are as below:
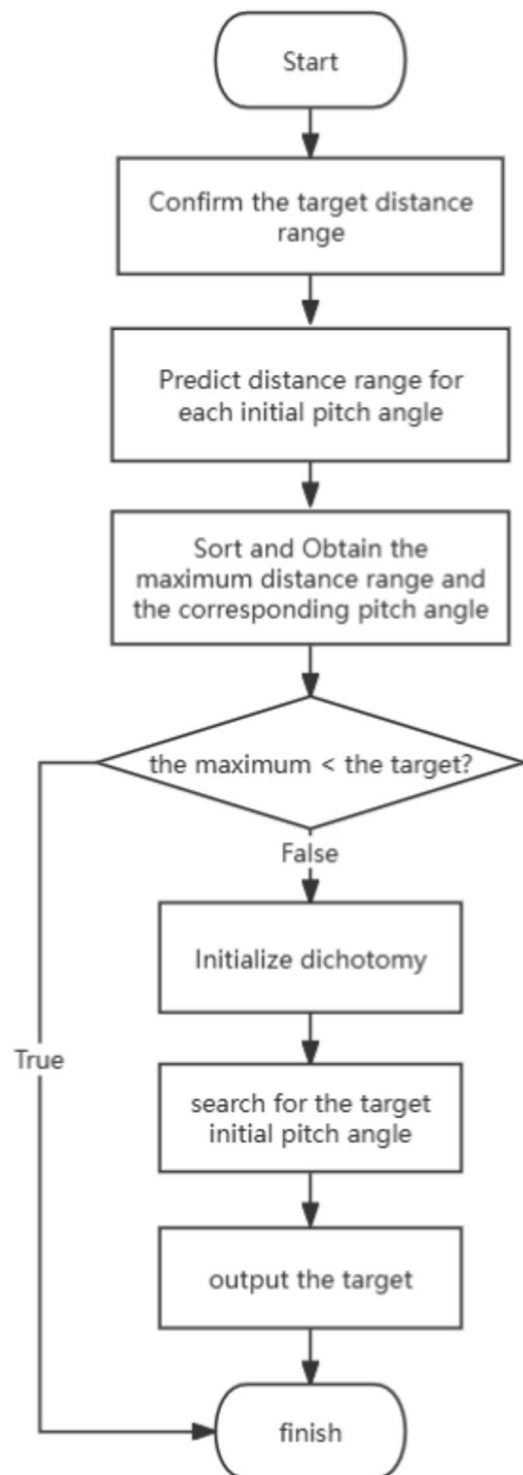

Fig. 5. Process of initial pitch angle computation.

- when jet ejects upwards, due to the double influence of gravity and air resistance, the velocity decreases fast, making it more easily for jets to crush into droplets, which weigh much lower than the jets. The lower weight, the more easily droplets are affected by air resistance, wind, and flow, which expands the loss of its velocity and thus affects the range. Normally, if ejection happens at a low initial height, greenery and buildings block the wind and air flow, which constructs a quite peaceful environment for jets. If ejecting at a higher place, jets lose the protection and are easily affected by the flow and wind.
- when jets eject downwards, due to the conflict between gravity and air resistance, the loss of velocity is slow. The core stable jets are mainly affected by the initial velocity, which is judged by working water pressure. Thus, the range is mainly about working water pressure.
- When the wind velocity is small, its effect on jets can be ignored; when it is big, it goes to the opposite.

Thus, considering the 3 things listed above, jet distance range is updated as:

$$\tilde{x} = x + \sum \beta_i \delta_i \tag{15}$$

where x represents the distance range computed by the model and is measured in meters, $\delta_i (i = 1, 2, 3)$ denotes the influence coefficient of height, working water pressure and wind respectively and thanks to the samples, Eqs. (16, 17 and 18) can be fitted respectively.

$$\delta_1 = x - \frac{h^2}{v_{out}} \tag{16}$$

where x represents the distance range computed by the model and is measured in meters, h represents the height range and is measured in meters, and v_{out} represents the initial velocity of jet and is measured in meters per second.

$$\delta_2 = x + (P_0 - P) \cdot x \tag{17}$$

where x represents the distance range computed by the model and is measured in meters, P_0 represents the rated working water pressure and is measured in mPa, and P represents the actual working water pressure and is also measured in mPa.

$$\delta_3 = x - \frac{h}{v_{wind}} \tag{18}$$

where x represents the distance range computed by the model and is measured in meters, h represents the height range and is measured in meters, and v_{wind} represents the actual wind velocity and is measured in meters per second.

The $\beta_i (i = 1, 2, 3)$ in Eq. (15) represents the influence respectively, and is defined as:

$$\beta_1 = \begin{cases} 1 & if \ h > H_0 > \epsilon \\ 0 & else \end{cases}$$

where ϵ represents the height threshold, H_0 denotes the initial ejecting height, unit in meters.

$$\beta_2 = \begin{cases} 1 & if \ \theta < 0 \\ 0 & else \end{cases}$$

where θ represents the initial pitch angle, unit in degree.

$$\beta_3 = \begin{cases} 1 & if \ v_{wind} > \omega \\ 0 & else \end{cases}$$

where ω represents the velocity threshold of wind, unit in meters per second.

			Distance range (unit: m)		Error	
h	θ_0	P	Experimental value (x)	Calculated value (x')	Δ (Unit:m)	relative Δ (Unit:%)
1.3	2.3	0.31	28.04	25.79	2.25	8.04
1.3	7.3	0.52	43.33	45.61	2.28	5.25
1.3	12.1	0.825	54.65	53.47	1.18	2.17
1.3	17.4	0.83	62.2	61.02	1.18	1.90
1.3	22.4	0.9	66.45	66.49	0.04	0.06
1.3	27.5	0.89	65	64.75	0.25	0.38
1.3	32.4	0.89	57.96	59.77	1.81	3.13
1.3	37.4	0.84	55	58.62	3.62	6.57
1.3	45	0.89	45.47	50.74	5.27	11.58
6.14	15.1	0.86	69	65.16	3.84	5.56
6.14	20.2	0.8	64.9	63.00	1.90	2.93
6.14	25.1	0.8	64.9	60.36	4.54	7.00
6.14	− 4.9	0.8	27.22	28.91	1.69	6.20
6.14	− 10.2	0.8	25.61	25.55	0.06	0.23
6.14	− 15.2	0.85	21.22	19.38	1.84	8.69
11.14	− 20.1	0.89	25.03	24.27	0.76	3.04
11.14	− 15.1	0.83	29.85	30.50	0.65	2.17
11.14	− 9.7	0.9	36.78	36.34	0.44	1.19
11.14	− 5.1	0.83	42.97	46.34	3.37	7.84
11.14	− 0.1	0.95	50.43	50.81	0.38	0.75
11.14	5	0.82	58.79	58.11	0.68	1.15
11.14	9.9	0.83	64.11	63.17	0.94	1.47
11.14	14.8	0.82	62.3	66.52	4.22	6.77
11.14	20	0.8	62.3	62.54	0.24	0.38
15.94	− 25.1	0.8	26.12	28.19	2.07	7.91
15.94	− 20	0.8	32.58	33.33	0.75	2.31

Table 2. Experiment samples and their calculations.

Computation of jet's initial pitch angle

So far, given an initial pitch angle, the landing point can be obtained by the model. However, practically, what has to be done is the inversion, which is targeting at the fire, measuring the distance, then setting an initial pitch angle and finally shooting. In other words, it is the initial pitch angle that has to be obtained and applied instead of a landing point.

Liu[16] obtained an analytical solution directly by the classical trajectory equation. However, getting an analytical solution is not a easy way for the proposed mode. this paper proposes an iterative solution with a searching algorithm which is searching an pitch angle that meets the requirements of height and distance.

As is illustrated in Fig. 4, under a certain working water pressure, when initial pitch angle is less than a certain value, the relationship between distance range and initial pitch angle is monotonically increasing, and when it is larger than the certain value, the distance range is to waver. Thus, there are multiple initial pitch angles satisfied with the distance range for a monitor under a certain water pressure and at a certain initial height. At the monotonically increasing period, distance range results cover all the areas that jets are able to reach. As a result, this paper uses dichotomy to search for the target initial pitch angle among angles involved in the period of monotonically increasing. As is shown in Fig. 5, the specific procedures are as below:

- Convert displacement x_{target} and L_0 to target distance range x:

$$x = x_{target} - L_0 \tag{19}$$

- Predict x_{pred} for every θ given the actual H_0 and the actual p, and obtain $\{x_{pred}|\theta, H_0, p, \theta \in (\theta_{min}, \theta_{max})\}$;
- Sort $\{x_{pred}\}$ and obtain the maximum $x_{pred_{max}}$ and the corresponding θ';
- If $x_{pred_{max}} < x$, then output *null* and finish; otherwise continue;
- initialize $low = \theta_{low}$ (θ_{low} is the minimum pitch angle that the cannon can reach) and $high = \theta'$, use dichotomy to obtain a θ_{target} satisfied with $|x_{pred} - x| < \epsilon$ (ϵ is a bearable error threshold) then output and finish. The dichotomy procedures are as below:

  - compute $\theta_{mid} = \frac{low+high}{2}$;
  - Retrieve x_{pred} corresponding to θ_{mid};
  - If $|x_{pred} - x| < \epsilon$, then $\theta_{target} = \theta_{mid}$ and finish; otherwise, continue;
  - If $x_{pred} < x$, then set low to θ_{mid}; if $x_{pred} > x$, then set $high$ to θ_{mid}, continue;

| h | θ_0 | P | Distance range (Unit: m) | | Error | |
			Experimental value (x)	Calculated value (x')	Δ (Unit:m)	relative Δ (Unit:%)
15.94	− 14.9	0.77	37.05	40.06	3.01	8.14
15.94	− 9.9	1	42.12	42.10	0.02	0.04
15.94	− 4.9	0.86	48.09	49.14	1.05	2.19
15.94	0.1	0.91	57.97	53.97	4.00	6.91
15.94	5.2	0.79	65.6	62.21	3.39	5.17
15.94	15.2	0.85	68.49	70.16	1.67	2.44
15.94	25.2	0.8	73.36	74.27	0.91	1.24
24.24	− 24.9	0.81	33.4	31.54	1.86	5.57
24.24	− 19.8	0.94	36.81	38.24	1.43	3.90
24.24	− 14.8	0.9	43.61	43.76	0.15	0.34
24.24	− 9.8	1	49.86	53.06	3.20	6.42
24.24	− 4.9	0.81	52.97	56.61	3.64	6.87
24.24	0	0.81	56.26	52.79	3.47	6.17
24.24	5.3	0.8	71	71.37	0.37	0.52
24.24	10.1	0.92	68.29	69.46	1.17	1.71
24.24	14.9	0.81	71.65	72.04	0.39	0.54
24.24	20.5	0.82	73.57	70.96	2.61	3.55
18.54	20.3	0.78	54.92	57.87	2.95	5.38
18.54	0.2	0.85	50.82	54.83	4.01	7.89
18.54	− 5	0.78	52.3	49.38	2.92	5.58
18.54	− 10.2	0.85	46.41	42.58	3.83	8.26
18.54	− 15	1.12	41.24	38.95	2.29	5.54
18.54	− 20	0.78	33.21	30.37	2.84	8.55
18.54	− 25.2	0.85	29.11	26.15	2.96	10.16
18.54	− 30.3	0.78	24.72	22.21	2.51	10.17
30.79	− 30.3	0.84	35.83	31.85	3.98	11.11
30.79	− 20.1	0.78	44.67	40.85	3.82	8.56
30.79	− 9.8	0.83	53.44	54.94	1.50	2.80
30.79	− 0.1	0.84	50.2	50.78	0.58	1.15
30.79	10.2	0.83	50.7	52.06	1.36	2.68
30.79	19.8	0.8	41.92	39.67	2.25	5.36

Table Tabnumbreak. .

Initial Ejecting Height (Unit: m)	Distance Range Change In Average (Unit: m/°)
1.30	0.97
6.14	0.68
11.14	0.91
15.94	0.96
18.54	0.74
24.24	0.90
30.79	0.50

Table 3. Sensitive analysis of distance range to initial pitch angle at different initial ejecting heights.

Experiments

This paper conducts experiments for a firetruck produced by Zoomlion and its model is JP65 on which the fire water monitor model is Akron 3480. The velocity at the nozzle inlet is the average velocity in the gun pipe, decided by working water pressure, working water discharge, rated water pressure and rated water discharge. Several corresponding parameters are as below:

- rated water discharge: the maximum of effective water discharge, and the value is $0.13\frac{m^3}{s}$;
- rated water pressure: the maximum of effective water pressure, and the value is 1.7 mPa;
- nozzle inlet diameter: the value is 100 mm;

Initial Ejecting Height (Unit: m)	Initial Pitch Angle Range	Distance Range Change (Unit: m/°)
1.30	≤ 0°	–
	0° − 10°	3.06
	10° − 20°	1.42
	20° − 30°	− 2.49
	≥ 30°	− 1.11
6.14	≤ 0°	0.59
	0° − 10°	–
	10° − 20°	4.82
	20° − 30°	0.00
11.14	≤ 0°	1.27
	0° − 10°	1.09
	10° − 20°	0.00
15.94	≤ 0°	1.09
	0° − 5°	1.50
	5° − 15°	0.39
18.54	≤ 0°	1.09
	0° − 20°	0.20
24.24	≤ 0°	0.92
	0° − 10°	1.18
	10° − 20°	0.52
30.79	≤ 0°	0.46
	0° − 10°	0.05
	10° − 20°	− 0.91

Table 4. Sensitive analysis of distance range to initial pitch angle range at different initial ejecting height.

Initial pitch angle	Distance range change in average (Unit: m/m)
−25°	0.63
−30°	0.45
−20°	0.52
−15°	1.05
−10°	1.02
−5°	1.19
0°	1.24
5°	0.69
10°	1.00
15°	0.75
20°	1.92
25°	0.43

Table 5. Sensitive analysis of distance range to initial ejecting height at different initial pitch angles.

Index	Model considering air resistance proportional to velocity	Model considering air resistance proportional to the square of velocity	Model this paper proposed
Average Error (Unit:m)	12.58	40.92	2.04
Average Relative Error (Unit:%)	24.53	81.62	4.55
Max Error (Unit:m)	52.66	64.94	5.27
Min Error (Unit:m)	0.09	13.48	0.02

Table 6. Prediction errors for each model.

- nozzle outlet diameter: the value is 89 mm;
- jet thickness: the value is 5 mm;
- the error threshold of searching for the target pitch angle: the value is 1 m;

For the convenience of testing and recording, truck conditions and operations are as below:

- In the interval of 1–31 m, every 5 m is used as an initial ejecting height;
- In the interval of -45 to $90°$, every 5 degrees is used as an initial pitch angle;
- Working water pressure is normally at 0.8 mPa, hence no change.

The distance range is measured by distance between the fire cannon and the center of core jet landing area.

Data from Table 2 comes from experiments and model calculation, in which H_0 represents the initial ejecting height, unit in meters; θ_0 represents the initial pitch angle, unit in degrees; P represents the working water pressure, unit in mPa; x represents the distance range that comes from the experiment, unit in meters; x' comes from the model calculation; Δ represents the difference between x and x'; relative Δ represents the percentage of Δ to x. The maximum x happens when the conditions are $H_0 = 24, 10 <= \theta_0 <= 20$ and $H_0 = 16, 15 <= \theta_0 <= 25$, which is around 70 m.

As is shown in Table 2, for different H_0, every 1 degree θ_0 changes, the variation of x is between 0.5 and 1, among which the largest variation happens when H_0 is between 10 to 25. Moreover, it can be seen in Table 3 that the distance range change varies among different initial pitch angle range even at the same initial ejecting height, and according to Table 3, normally, for all initial ejecting height, when initial pitch angle range increases to a value, the distance range change starts to decrease, which matches to the computation result illustrated by Fig. 4. Moreover, it also varies among different initial ejecting height in a same initial pitch angle range. For example, the range from 0 to 10 of θ_0 is the most sensitive range in the ranges at 1.30 m high for x changing, while the most sensitive initial pitch angle range is from 10 to 20 when the initial ejecting height is 6.14 m. Table 4 shows a sensitive analysis result which is that among all θ_0, every 1 meter H_0 changes, x changes from 0.4 to 1.9. And, θ_0 ranges with large x variations are -15 to $0°$ and 10 to $20°$.

To conclude, x is influenced by both H_0 and θ_0, and the influence is non-linear. Practically, to improve efficiency, it is best to choose a θ_0 range which makes x change greatly but the sensitivity is low, such as the range from -15 to $0°$, which is also the range this paper is to search in. Choosing a proper H_0 with the θ_0 makes jets land just at the target.

As is shown in Table 5, maximum prediction error of the model considering air resistance proportional to velocity reaches 53 m and the average relative error is 24.5%, though it is still less than the value of the model considering air resistance proportional to the square of velocity, of which the maximum prediction is 65 m and the average relative error is 81.6%. Nevertheless, the proposed model makes the maximum prediction error within 5 m, average in 2 m, and the relative error decreases to 4.6%.

Conclusion

This paper researches on water jet trajectory and landing point prediction anchored by monitor's initial pitch angle solution, realizing an automatic system for monitor to aim at the target without human involving and thus improving firefighting efficiency.

Considering the crushing and atomization of water jets and also air resistance, wind and height, this paper proposes a core stable jet definition, adapts it to predict the landing point and makes some compensation for the prediction, which limits the distance error within 4.6%, which is satisfied for the engineering application and help achieve intelligent fire monitor. This proposed model costs 0.00292 s for each computation in average, obviously less than the prediction of neural network and of hydrodynamics cost.

Regarding to the complexity and variability of the actual situation, experiments in this paper still don't cover all the situations in the world, such as in forests, and they just cover some typical situations in city. Hence, in the future, the jet trajectory model and landing point prediction method is going to be updated.

Data availability

All data generated or analysed during this study are included in this published article.

References

1. Jiao, L., Yang, S., Liu, F., Wang, S. & Feng, Z. Beyond neural networks: Retrospect and prospect. *Chin. J. Comput.* **39**, 1697–1716 (2016).
2. Zhang, C., Zhang, R., Dai, Z., He, B. & Yao, Y. Prediction model for the water jet falling point in fire extinguishing based on a GA-BP neural network. *PLoS ONE* **14**, e0221729. https://doi.org/10.1371/journal.pone.0221729 (2019).
3. Lin, Y., Ji, W., He, H. & Chen, Y. Two-stage water jet landing point prediction model for intelligent water shooting robot. *Sensors*[SPACE]https://doi.org/10.3390/s21082704 (2021).
4. Tang, J. *Study on Cutting Model for Abrasive Water Jet Based on Artificial Neural Network*. Master's thesis, Xihua University (2011).
5. Wang, F., Chen, X., Min, Y. & Wang, W. Fitting model of water jet track of fire monitors. *Fire Sci. Technol.* 656–658 (2007).
6. Liao, X., Liu, P. & Chen, W. Study on fire monitor's jet track based on matlab. *Fire Sci. Technol.* **33**, 1169–1172 (2014).
7. Chen, X. & Yang, Y. Jet trajectory model and positioning compensation method for fire water cannon. *Chin. J. Eng. Des.* **23**, 558–563 (2016).

8. Min, Y., Chen, X., Chen, C. & Hu, C. Pitching angle-based theoretical model for the track simulation of water jet our from water fire monitors. *Chin. J. Mech. Eng.* **47**, 134–138 (2011).
9. Sun, J. *Research of the trajectory of fire-fighting monitor's Jet.* Master's thesis, Shanghai Jiao Tong University (2010).
10. Zhu, J. *Research on Intelligent Fire Monitor Control Based on Machine Vision.* Ph.D. thesis, China University of Mining and Technology (2021).
11. Hao, W. *Modeling and control of water jet for forest fire truck.* Master's thesis, Beijing Forestry University (2020).
12. Wan, F. *The analysis on the jet track and positioning performance of the fire monitor.* Master's thesis, Shanghai University (2008).
13. Wang, K., Guo, L. & Yang, W. A methodology to position jet landing point of fire monitor and the fire-fighting robot (2016).
14. Wang, Y., Li, C. & Zhang, J. Automatic controlling method to jet for aerial fire vehicles (2020).
15. Liu, X., Zhang, M. & Liang, Z. Method to confirm landing point of fire monitor water jet (2018).
16. Liu, B., Chen, Y. & Ren, S. Method to calculate jet pitch angle of auto tracking and targeting jet suppression system (2014).

Author contributions

Q.F., Q.D. and Q.L. conceived and designed the experiments. Q.L. analyzed the data. All authors interpreted the results. Q.F. and Q.L. wrote the first and revised drafts of the manuscript. All authors contributed to the manuscript and reviewed the manuscript. All the authors agreed with the results and conclusions of the manuscript.

Competing interests

The authors declare no competing interests.

Additional information

Correspondence and requests for materials should be addressed to Q.F.

Reprints and permissions information is available at www.nature.com/reprints.

Publisher's note Springer Nature remains neutral with regard to jurisdictional claims in published maps and institutional affiliations.